EXHIBIT B

Min Invas Ther & Allied Technol 2000: 9(1) 107–118

Optimisation of processing and properties of medical grade Nitinol wire

A.R. Pelton[1], J. DiCello[1] and S. Miyazaki[2]

[1]Cordis Corporation – Nitinol Devices and Components, Westinghouse Drive, Fremont CA, USA; and [2]Institute of Materials Science, University of Tsukuba, Ibaraki, Japan

Summary

The purpose of this paper is to review the current processing and resultant properties of standard Nitinol wire for guide-wire applications. Optimised Ti-50.8at%Ni wire was manufactured according to industry standards by precise control of the composition, cold work and continuous strain-age annealing. Mechanical properties of this wire are reported from −100°C to 200°C to demonstrate the effects of test temperature. Within the 'superelastic window' the plateau stresses are linearly related to test temperature. Additional ageing treatments can be used as a tool to fine-tune transformation temperatures and mechanical properties. A review of the fatigue properties of thermomechanically-treated Nitinol wire shows that they are affected by test temperature, stress and strain.

Keywords

Nitinol, shape-memory, superelasticity, mechanical properties, ageing, fatigue

Introduction

The growth in the use of Nitinol in the medical industries has exploded over the past 10 years. Patients and care-providers have encouraged the transition from traditional open-surgical procedures that require long hospital stays, to less-invasive techniques, which are often performed in out-patient facilities [1]. This demand for minimally-invasive procedures has required novel instrumentation and implants to be designed by engineers and physicians. An increasing number of these devices use Nitinol as the critical component. Examples of these medical applications are richly illustrated in companion articles in this journal [2,3], and range from endoscopic instruments to implants, such as stents and filters. It is interesting that the majority of these devices depend on mechanical superelastic behaviour, which is a significant departure from the original thermal shape-memory industrial uses of Nitinol.

Since the 'discovery' of the shape-memory effect in TiNi alloys in the 1960s, metallurgists have investigated methods to control transformation temperatures and mechanical properties through alloying additions, improved melting practices and thermomechanical processing (see, for example, References 4 and 5). The production of many thousands of kilometers of wire for such diverse products as cellular telephone antennae, eyeglass frame components, guidewires, undergarment supports and orthodontic archwires profoundly influenced the acceptance of Nitinol in the marketplace. These commercial opportunities have allowed Nitinol suppliers to focus on improving

Correspondence: A. Pelton, *Cordis Corporation – Nitinol Devices and Components, 47533 Westinghouse Drive, Fremont CA 94539, USA.*

processes for a few standard alloys, rather than pursuing a myriad of 'boutique alloys' with niche applications. The composition and processes have been refined so that, for example, the transformation temperature in final products is routinely controlled to within ± 3°C. More recently, the availability of seamless tubing and sheet have provided designers with additional tools to solve engineering problems. Furthermore, microfabrication techniques, such as laser machining [6] and photoetching [7], have also contributed to the increase in the number of miniature devices made from Nitinol.

Accordingly, Nitinol properties have become very predictable, which is a basic requirement of design engineers. As the Nitinol industry has matured over the past two decades, terms such as 'shape-memory', 'superelasticity', 'recovery forces', 'plateau stresses', and 'transformation temperatures' are now recognised by more than just a select few metallurgical specialists. Although design engineers have a good understanding of the basic properties of the alloys, they still have many good questions. Typically these include:

- Are the mechanical properties constant over a wide range of temperatures?
- Can we adjust the transformation temperature without modifying the mechanical properties?
- Do the shape-memory and superelastic properties imply that Nitinol has an infinite fatigue life?

The purpose of this article is to address these questions by reviewing the processing and resultant properties of Ti-50.8at%Ni wire that has been manufactured for medical guide-wire applications. Furthermore, this article will focus on the effects of standard continuous thermomechanical processes, rather than long-term 'batch' processing, which was more common in the 1970s and 80s.

Processing

Optimisation of the superelastic properties of Nitinol for a specific product is achieved through a combination of cold work and heat treatment. The first step in optimising the thermomechanical treatments of wire and tubing products is to draw the material through a series of dies, to achieve 30–50% reduction in cross-sectional area [8]. Past methods have employed a long-term batch annealing process but, to attain a more uniform product, continuous strand strain annealing is the most effective method. With this method, the Nitinol wire is under constant strain during the annealing process. Continuous 'strain annealing' ensures that the entire spool will be processed with the identical thermomechanical treatment, resulting in a product with uniform properties from end to end.

Figure 1 shows a typical continuous-strand strain straightening process line.

Continuous-strand straightening usually occurs in a temperature range of 450–550°C under a stress of 35–100 MPa. As the wire moves into the heat zone it will initially want to shrink in length and grow in diameter, due to the shape-memory effect not suppressed by the cold work of the drawing process (springback). The wire temperature quickly increases, its strength will drop and the applied strain will straighten the wire and, depending on the strain, reduce the wire diameter slightly. In the continuous process it is difficult to measure the active strains during straightening as they occur inside the furnace. However, the following vertical straightening example can help define the strains operating during the continuous process.

During vertical straightening of discrete lengths of wire, the wire is heated via electrical resistance and is therefore exposed to make visible measurements. As a 1.5 mm diameter wire was being electrically straightened, it showed a maximum springback of 1.2% during heating and a 2.4% extension strain at the end of the straightening cycle. Similar strains would be expected with the continuous-strain straightening method.

Straightness, mechanical properties and the active A_f are all affected by the speed and temperature parameters of the straightening process. As with all thermally-activated processes, time at temperature controls the final properties of the wire. More time at temperature softens the wire and moves its mechanical properties toward a fully annealed product, while short times leave the material closer to the high strength cold-worked state. To optimise the superelastic properties, a balance must be developed between these two extremes. The requirements of

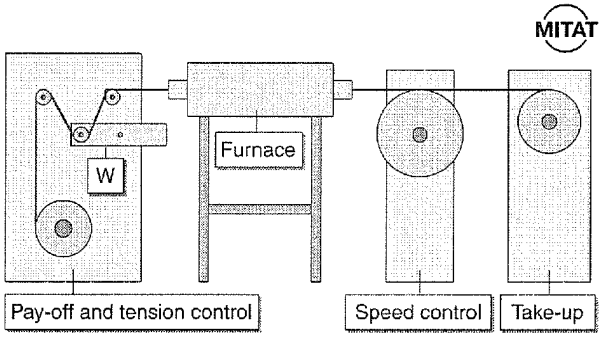

Figure 1. Schematic diagram of a continuous strand annealing equipment for optimised production of Nitinol superelastic wire.

the final product will help define the process parameters. A high torqueable guide-wire may require slower speeds than a high strength wire that has a table-roll straightness requirement. Additional speed and temperature adjustments may be necessary to meet any active A_f requirements (see discussion below) as well.

Properties

In this section we will consider the methods of characterising the thermal and mechanical properties of thermomechanically-processed wire. The focus will be on products that are superelastic between room temperature and body temperature. We will document the mechanical properties from −100°C to 200°C, to illustrate how test temperature affects performance. Furthermore, since many wire and tubing products are given additional thermal shape-setting, we will establish the effects of ageing time and temperature treatments on transformation and mechanical properties. Finally, since many Nitinol medical devices are used in (human) fatigue environments, we will discuss the influence of strain amplitude and test temperature on bending fatigue behaviour.

Transformation temperatures

Harrison [9] cataloged >20 techniques that have been used to measure the changes associated with the shape-memory transformation. Two of the most fundamental ways to determine the **qualitative** transformation temperature involve sound and feel. Even a novice can distinguish between the 'ping' from austenite and 'thud' from martensite when dropped on the floor. Although this is not a highly quantitative means to measure transformation temperatures, it has been used to sort alloys quickly without sophisticated equipment. Another qualitative method is to feel the alloy. Martensite 'feels' rubbery when bent, whereas austenite feels 'springy'.

These two simple examples cited above illustrate that the martensitic transformation affects a variety of properties. However, Harrison [9] offered the sage advice that the chosen measurement technique should parallel the actual function of the product. For example, many medical customers request certification of the A_f temperature to ensure that the product is austenitic above a certain application temperature. These customers generally specify that the measurements are obtained by either differential scanning calorimetry (DSC) or free recovery ('active') techniques. DSC measures the heat released and absorbed during the martensitic (exothermic) and austenitic (endothermic) transformations, respectively [10, 11]. Free recovery, however, is by far the most simple and often the most useful method to measure A_f. This technique only requires the following steps, which simulate a shape-memory cycle:

- cool to a low temperature (for example in a cooled alcohol bath);
- bend the sample to a prescribed strain (2–3%);
- watch and record the temperature at which the sample returns to its original shape when heated: this is defined as the A_f temperature.

Free recovery can also be instrumented in order to obtain a permanent record of the results [12, 13]. Both of the above techniques have the benefit that they are straightforward to conduct, amenable to use for small specimens, require minimal sample preparation (especially free recovery) and are reproducible.

Figure 2 compares the DSC thermogram and instrumented free-recovery measurements from the same wire. The DSC records the heat flow during both cooling and heating, whereas free recovery records the deflection recovery only during heating. The key transformation temperatures, martensite start (M_s), martensite finish (M_f), austenite start (A_s) and austenite finish (A_f), are marked as appropriate on both charts. Also included are atomic models of the austenite (cubic structure) and martensite (monoclinic structure) to help the reader visualise the transformations.

Note that the DSC graph shows an R-phase peak during cooling from a high temperature. Although an in-depth discussion of the R-phase is beyond the scope of this paper, it is important to point out that the R-phase is another shear transition in competition

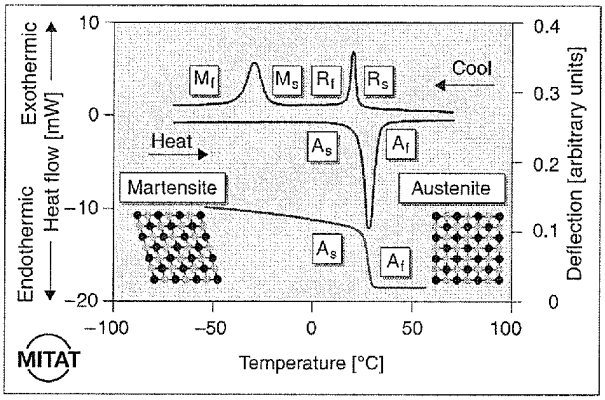

Figure 2. Differential scanning calorimetry and free recovery of the same processed wire. Note that upon cooling the wire transforms to R-phase prior to the martensitic transformation. Upon heating, both techniques provide similar A_s and A_f temperatures as the (monoclinic) martensite transforms to the (cubic) austenite.

with martensite [14]. In the case shown in Figure 2, the R-phase forms around room temperature. With further cooling, the martensite transformation begins at about −23°C (M_s) and is fully martensitic below −38°C (M_f). When the sample is reheated, the reverse transformation begins at about 22°C (A_s) and finishes at an A_f of 32°C. Note that there is a wide hysteresis between the M_f and A_f, which is characteristic of shape-memory alloys. The origin of the hysteresis is attributed to microscopic internal friction effects [15]. The A_s (24°C) and A_f (32°C) data from the free recovery method are nearly identical to those from DSC.

Mechanical properties

Based on the transformation behaviour shown in Figure 2, the wire should be fully austenitic above 32°C. However, an important characteristic of shape-memory alloys is that stress can trigger the martensitic transformation at temperatures above A_f (the 'thermoelastic' effect [15]). From a thermodynamic viewpoint, this means that it is easier (lower free energy) for the wire to create martensite in response to the applied stress than to deform plastically (dislocation formation) [15,16]. Stress-induced martensitic transformations can be easily understood by considering Figure 3 [17]. This diagram compares atomic motions in response to an applied stress by traditional Hookian elastic (top) and transformational superelastic (bottom). For Hookian elasticity, which represents conventional materials, such as stainless steel, the atomic bonds 'stretch' up to about 0.5% before plasticity occurs. In contrast, the austenitic structure depicted on the bottom left structure transforms into martensite with applied stress. As the magnitude of the stress increases from left to right, the amount of martensite increases. Up to 10% strain can be accommodated by stress-induced martensitic transformations. The martensitic structure formed by superelasticity is identical to that formed through the shape-memory process, as illustrated in Figure 2.

Figure 4 is a schematic stress–strain curve that corresponds to this model of transformational superelasticity. When the wire is pulled beyond its Hookian elastic limit (approximately 1.5% strain in Nitinol), there is an apparent 'yield' at a critical stress. Atomistically, this is represented by the onset of martensitic transformation, as shown in the second diagram in Figure 3. The wire can be further stretched at a relatively constant stress along the 'loading plateau' until the entire structure has transformed into martensite. As the stress is removed, the martensite immediately recovers elastically (linear unloading) and then begins to revert back to austenite on the 'unloading plateau'. The ability of the material to return to its original shape when the stress is released is an important attribute for many products,

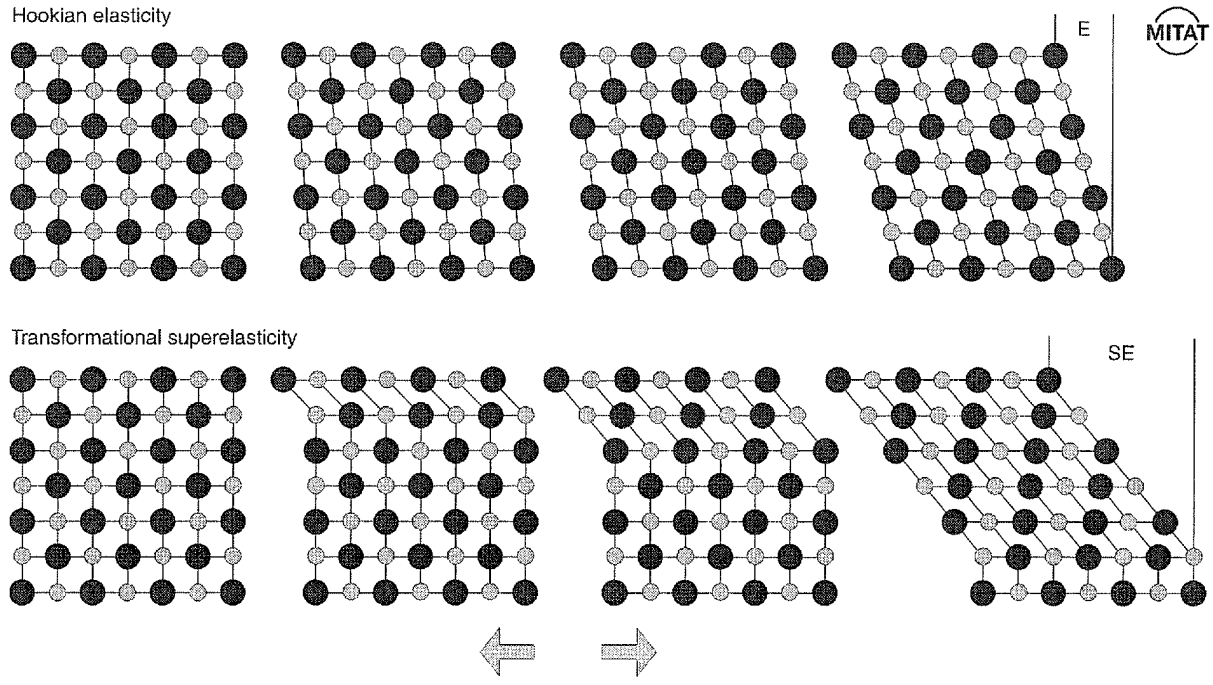

Figure 3. Schematic representation of the atomic motions associated with Hookian elasticity observed in conventional materials and transformational superelasticity of Nitinol. (From Stöckel and Yu, Ref. 17.)

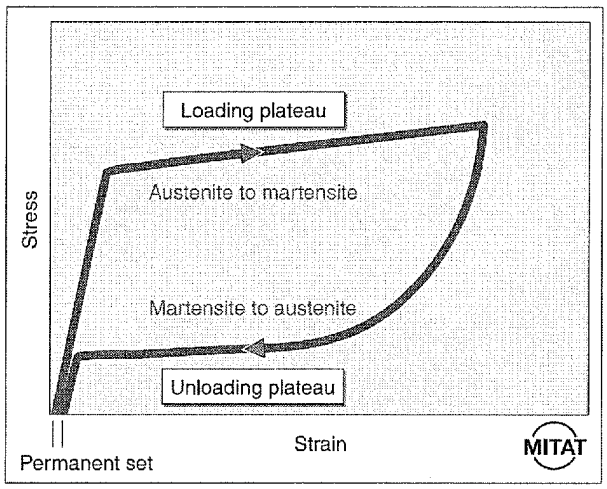

Figure 4. Schematic stress–strain curve of superelastic Nitinol. There is a transformation from austenite to martensite that begins at the apparent yield stress. The plateau stress remains nearly constant with increasing strain as the amount of martensite increases. Upon unloading, the martensite reverts to austenite along the unloading plateau. The 'permanent set' measures any residual strain.

such as guide-wires, to minimise kinking. Any residual strain is caused by an accumulation of plastic strain and is measured by the 'permanent set', as shown on the figure. Note that the stress–strain curve exhibits a stress hysteresis that, similar to the thermal hysteresis discussed above, is due to microstructural frictional effects. The magnitude of the stress hysteresis plays an important role in the design of many Nitinol applications, such as Nitinol eyeglass frames. A high loading stress is required to resist easy bending of the frame, whereas the unloading stress should be low so that the temples exert a gentle pressure against the head. Stöckel [2] discusses other examples of this 'biased stiffness' property.

Effects of test temperature

The tensile curves shown in Figure 5 illustrate that the mechanical behaviour of Nitinol varies greatly from −100°C to 150°C. In these tests, wires with an A_s of −22°C and A_f of 11°C were pulled to 6% strain, unloaded to zero stress and were then pulled to failure. At the lowest test temperatures, the wires are martensitic and the high residual strains are fully recovered by heating above A_f (the shape-memory effect). From about 0°C to 100°C the tensile curves exhibit superelastic 'flags', and we note that it becomes more difficult to stress-induce martensite as the test temperature increases. Along with the increase in the plateau stresses, the permanent set also increases with temperature. The tensile behaviour at 100°C, with a high permanent set, but a well-defined unloading curve, indicates that deformation is accommodated by a combination of stress-induced martensite and conventional plasticity. Above 150°C, however, the wire deforms by plastic mechanisms rather than martensitic transformations, which results in a linear unloading curve. The temperature where it is too difficult to stress-induce martensite is defined as M_d; in the present case, M_d is between 100°C and 150°C.

The effects of test temperature on the tensile curves shown in Figure 5 may be further analysed by considering each of the key attributes. For example, Figure 6 shows the temperature dependence of the permanent set from these wires after unloading from 6% strain. At lower temperatures, the unresolved strain is due to deformation of the martensite, and can be recovered by heating above A_f. The residual strain is nearly zero between 0°C and 60°C, which defines the superelastic 'window' for this alloy. As noted above, the non-recoverable plastic strain is about 1 % at 100°C and then increases to about 3 % at 150°C. Many medical applications require superelastic behaviour between room temperature and body temperature. Therefore, this 60°C window is perfectly centered about the intended application range.

Figure 7 shows the effects of test temperature on the loading, unloading and ultimate tensile stress. We see that there is a linear relationship between plateau stress and temperature between about 0°C and 60°C for the unloading plateau and up to 150°C for the loading plateau. These variations in plateau stress follow the Clausius–Clapeyron relationship for a first-order transformation [16]:

$$\frac{d\sigma}{dT} = \frac{-\Delta H}{T\varepsilon_0}$$

Where $d\sigma$ is the change in plateau stress, T is the test temperature, ΔH is the latent heat of transformation (obtained from DSC measurements), and ε_0 is the transformational strain. ΔH and ε_0 are controlled by the crystallography of the transformation and can be considered constants. The right side of the equation therefore defines the 'stress rate' for the stress-induced transformations. For the present case, the stress rate is 6.1 MPa°C^{-1}, which is within the typical range of 3–20 MPa°C^{-1} for Nitinol alloys [18]. The consequence of this relationship is that the mechanical properties of Ti–Ni alloys depend directly on the transformation temperature and test temperature.

The ultimate tensile stress (UTS) gradually decreases from approximately −100°C to 150°C, with a slight minimum at 150°C. The UTS and plateau

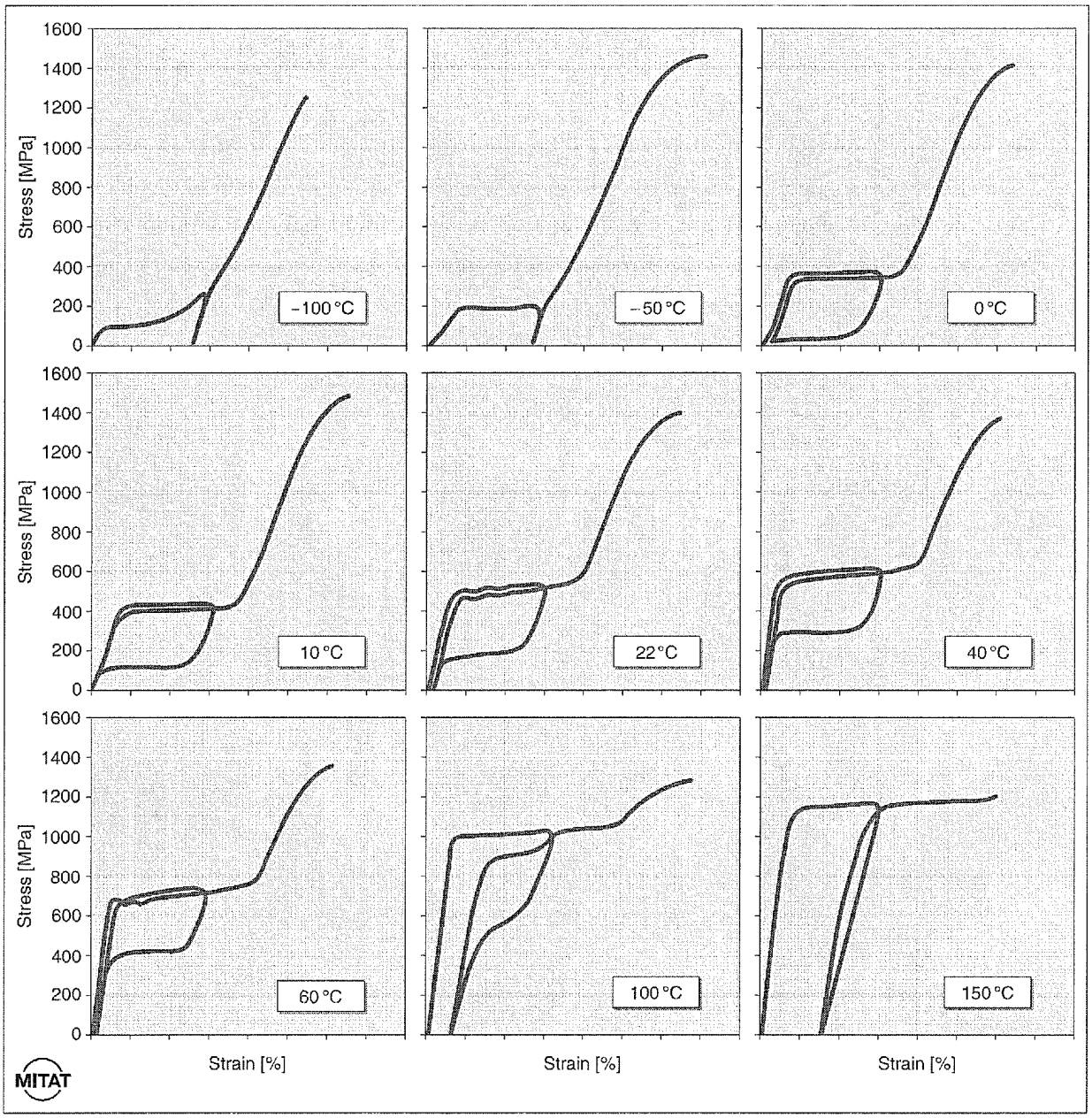

Figure 5. Effect of test temperature on the mechanical behaviour of Nitinol wire. Note that there is a systematic increase in the loading and unloading plateau stresses with increasing test temperature. Below 0°C, the structure is martensite and, above 150°C, the graph shows conventional deformation of the austenite. The intermediate temperatures all show classic transformational superelasticity.

stress converge above this temperature, which is a further indication that M_d is near this temperature. In Figure 8, we see that the elongation is fairly constant up to about 150°C and then drops at the higher temperatures. The combination of the low ductility and high stresses above 150°C may indicate a toughness minimum for this material.

Effects of ageing heat treatments

Several investigators have shown that optimal superelastic performance can be achieved in Nitinol alloys that have a combination of cold work and ageing heat treatments [18, 19]. Precise control of these thermomechanical treatments can lead to reproducible mechanical properties and transformation temperatures. TiNi alloys with 50.8% Ni respond well to ageing heat treatments to 'tune in' the

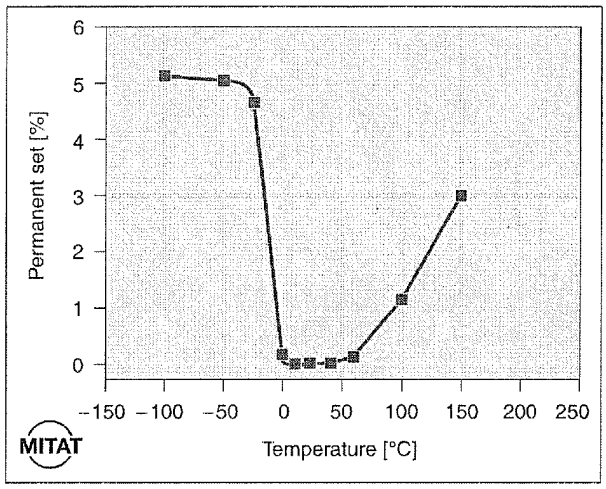

Figure 6. Effect of test temperature on permanent set is shown from the data in Figure 5. The 'superelastic window' extends from approximately 0°C to 60°C, where there is minimal residual strain after unloading from 6 % strain. Below 0°C, the strain can be recovered by heating above A_f = 11°C (the shape memory effect) and at higher temperatures the residual strain is due to plasticity.

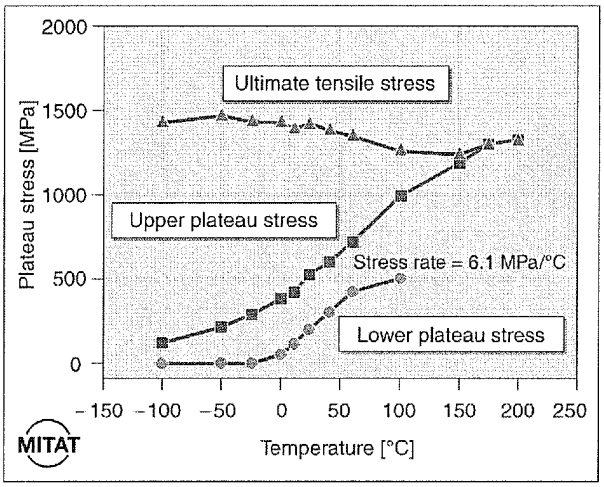

Figure 7. Effect of test temperature on plateau and tensile stresses is shown from the data in Figure 5. Note that there is a linear relationship between plateau stress and test temperature from about 0°C to 100°C with a slope, or stress rate of 6.1 MPa/°C^{-1}. The ultimate tensile stress shows a gradual decrease with increasing temperature with a minimum at the M_d of 150°C.

desired properties. Nishida *et al.* [20] established the effects of ageing time and temperature on the Ti-Ni precipitation reactions in Ti-51%Ni alloys by metallographic methods. They observed precipitation sequence of $Ti_{11}Ni_{14}$ – Ti_2Ni_3 – $TiNi_3$ in the TiNi matrix at temperatures between 500°C and 800°C and for times up to 10 000 h and presented the data in a time–temperature–transformation (TTT) diagram. Their

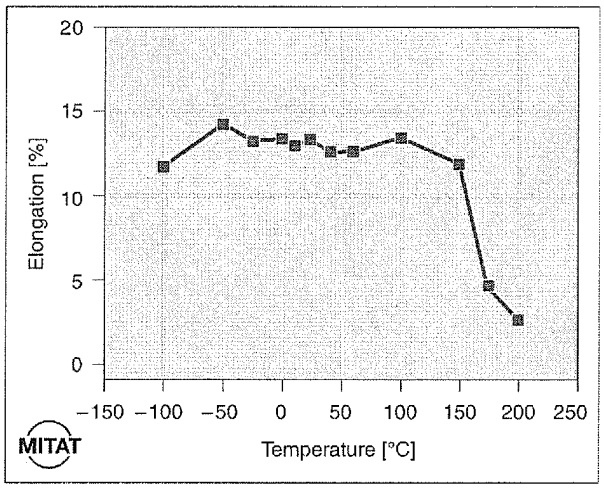

Figure 8. Effect of test temperature on elongation is shown from the data in Figure 5. The elongation does not vary much with temperature up to approximately 150°C. The drop in ductility at the high temperatures may signify a toughness minimum.

work gave great insight into the metallurgical tool of controlling precipitation reactions in Nitinol alloys.

Clearly, however, the times investigated by Nishida *et al.* [20] are significantly longer than can be tolerated in a production environment. Therefore, straight wires from the previous section were aged between 300°C and 550°C for 2 – 180 min, to characterise the effects on transformation temperature and mechanical properties. Figure 9 illustrates these effects on the A_f temperature. We note that the transformation temperature does not change significantly at 300°C. Also, at 500°C, the A_f increases slightly at short times, but does not increase rapidly. The intermediate temperatures, namely 350 – 450°C, have a greater impact on the transformation temperature. At the highest ageing temperature, 550°C, there is an initial decrease in A_f and then a rapid increase. Admittedly, these trends of temperature and time on the A_f may appear counter-intuitive. However, more clarity is gained by grouping the time–temperature conditions to obtain common A_f temperatures. Figure 10 is such a TTT diagram, where each 'c-curve' represents the loci of constant A_f. This figure illustrates that there is a maximum in the precipitation reaction at about 425°C; i.e., the A_f increases most rapidly after heat treatments at 425°C. For example, the A_f increases from 11°C in the as-straightened wire, to 30°C after ageing for only 10 min. To reach the same 30°C A_f at 500°C takes about 60 min and at 300°C the time exceeds 180 min.

It is certainly beyond the scope of this article to review the metallurgy of precipitation reactions. However, the shape of these curves can be understood

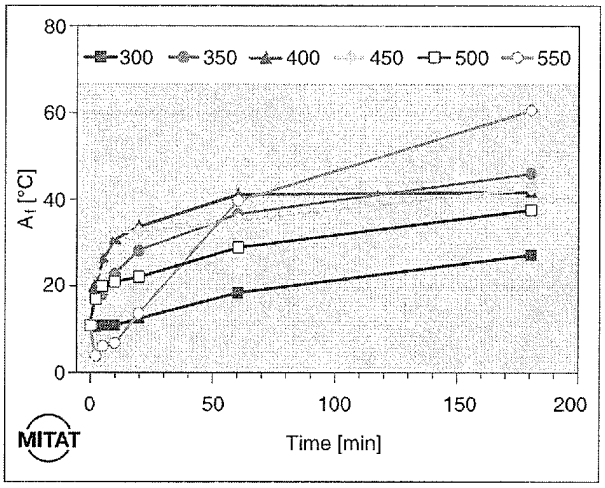

Figure 9. Effect of ageing temperature and time on the transformation temperature of Ti-50.8% Nitinol wire with a starting A_f temperature of 11°C are shown. Note that all of the ageing temperatures tend to increase the transformation temperature, although at 550°C there is an initial decrease.

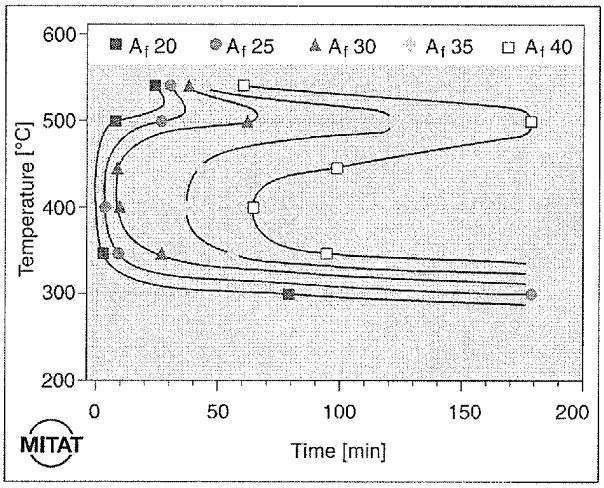

Figure 10. Effect of ageing temperature and time on the transformation temperature of Ti-50.8% Nitinol wire with a starting A_f temperature of 11°C are shown. The data from Figure 9 are re-plotted to illustrate the conventional time–temperature–transformation (TTT) diagram. Note that the maximum precipitation rate is about 400°C. Between 500°C and 550°C the precipitates dissolve and tend to lower the A_f. A new precipitate forms at 550°C (see text for more details).

by briefly exploring two factors that govern diffusional nucleation and growth of precipitates [21]. At high temperatures, there is sufficient thermal energy to permit rapid diffusion of Ni and Ti atoms in the matrix. However, it becomes more difficult for the atoms to form a precipitate nucleus as the temperature increases. At lower temperatures, however, just the opposite situation occurs: here we have high nucleation rates, but low diffusion rates. These two processes are optimised at the intermediate temperatures (350 – 450°C) to achieve maximum precipitation rates. The A_f change, therefore, is due to relative Ni and Ti atom diffusion, where the Ni atoms congregate in the precipitates and the Ti atoms move to the TiNi matrix phase. As the matrix becomes enriched in Ti, the transformation temperature increases, as expected from the relationship of composition to transformation temperature [22]. Although the overall composition of the material remains Ti–50.8% Ni, localised shifts of composition can affect the transformation temperatures.

The trends in the TTT curves indicate that a single precipitation reaction ($Ti_{11}Ni_{14}$) occurs in the temperature range 300–500°C. Between 500°C and 550°C, however, there are 'cusps' in the A_f curves. Above 500°C, the $Ti_{11}Ni_{14}$ precipitates dissolve and there is a corresponding **decrease** in the transformation temperature, as the Ni atoms diffuse back into the matrix. At 550°C the Ti_2Ni_3 phase precipitates require an even greater amount of Ni to diffuse away from the matrix. Precipitation of this phase, therefore, will again increase the A_f, but at a different reaction rate than for $Ti_{11}Ni_{14}$. These findings are consistent with Miyazaki's microstructural study of Ti-50.6%Ni alloys after ageing for 60 min at 400°C, 500°C and 600°C [19]. His results demonstrate that the maximum density of $Ti_{11}Ni_{14}$ precipitates is obtained at 400°C.

The effects of the ageing treatments on the loading plateau stress are shown in Figure 11. Since the wire was 'strain-aged' during the initial processing, these additional ageing treatments do not increase the loading plateau. Ageing temperatures in the 300–500°C range systematically decrease the loading plateau, as we would expect with the increase in A_f temperature. At 550°C, there is an initial decrease in loading plateau stress and then a more rapid decrease as ageing and annealing processes occur. The effects of ageing on the UTS are more interesting, as seen in Figure 12. Here the ageing treatments between 300°C and 450°C increase the UTS. This illustrates that the $Ti_{11}Ni_{14}$ precipitates are effective barriers to dislocation motion. Although we know that precipitates form during ageing at 500°C and 550°C, there is a dramatic decrease in UTS, especially at 550°C. The decrease in plateau and tensile stress at 500°C and 550°C illustrates that this is an effective temperature range for annealing (dislocation annihilation).

The above ageing discussion points out that the transformation temperature can be readily adjusted by

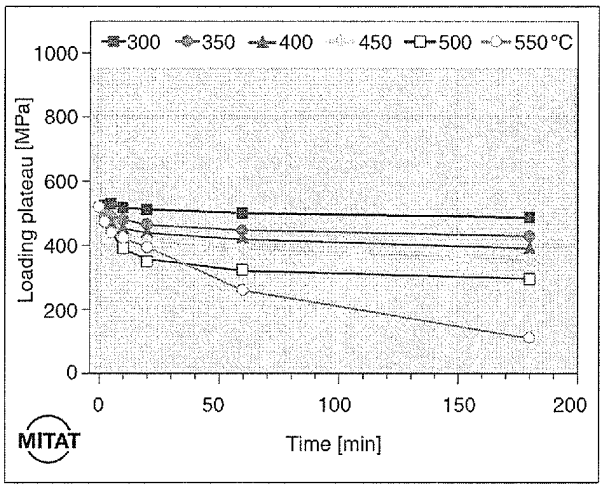

Figure 11. The effect of time and temperature on the loading plateau of aged Ti-50.8% Nitinol alloy. These stress data correspond to the A_f temperatures shown in Figures 9 and 10. There is a systematic decrease in plateau stress with increasing temperature. There is a more dramatic effect at 550°C.

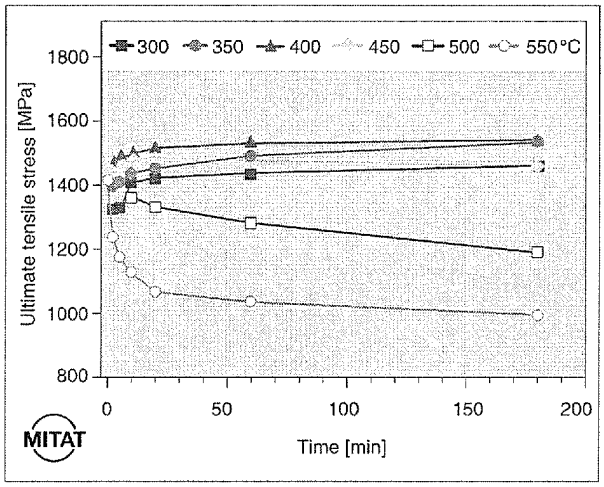

Figure 12. The effect of time and temperature on the ultimate tensile stress. Ageing temperatures between 350°C and 450°C tend to increase the tensile strength due to precipitation hardening. At 500°C and 550°C, the annealing effects dominate and lower the strength.

selecting an appropriate time and temperature. Higher A_f temperatures are achieved by ageing in the 300 – 500°C range. Additionally, the A_f can be lowered by short ageing times between 500 and 550°C.

Fatigue properties

Fatigue life is a major concern for biomedical implant applications. For example, the US FDA requires proof of fatigue resistance of 10 years (400 million cycles) in simulated body environment for intravascular stents [23]. Pedersen *et al.* [24] measured 6% average diametral strain in proximal aorta at 100 mmHg pressure differential. Therefore, an implanted device could be exposed to pulsatile strains as high as 6%. The actual mean strain that the implant is subjected to depends on material and design factors. However, whether the stent is manufactured using woven wire, etched sheet, or laser-cut tubing, the strut sections undergo cyclic bending deformation. Although several papers have reported on the fatigue properties of Ti–Ni alloy plates and bars [25] under tension–compression conditions, only a few recent papers have been published on the fatigue life of Ti–Ni wires [26, 27]. Furthermore, many Nitinol products are tested under accelerated pulsatile conditions that allow only periodic observations to ensure that the devices have not fractured (for example, see Reference 28). A logical approach, however may be to supplement these 'submission tests' with more fundamental bend–fatigue studies on wires or stent elements to aid in the design phase. The purpose of the present section, therefore, is to review the effects of strain amplitude, stress and test temperature on the fatigue life of binary Ti–Ni alloy wires.

Miyazaki *et al.* tested cold-worked and aged Ti-50.0at%Ni [27] and Ti-50.9at%Ni [28] wires in a rotary-bend apparatus. The specimens were fixed in a bent shape with a suitable radius of curvature to induce a desired strain at the specimen surface at specified temperatures above and below A_f. Figure 13 shows the (outer fibre) strain amplitude (ε_a) versus number of rotations to fracture (N_f) relationship at each test temperature for the two alloys. The upper diagram shows three curves for the Ti-50.9at%Ni alloy and the data for the Ti-50.0at%Ni alloy is in the lower diagram. Both alloys show a general trend of increasing fatigue life with decreasing test temperature in the highest and intermediate strain-amplitude regions. In the higher Ti alloy the fatigue-endurance limit increases with decreasing temperature below A_f. The fatigue limit is insensitive to temperature for the Ti-50.0at%Ni alloy above A_f and for all conditions for the Ti-50.9at%Ni.

Miyazaki *et al.* [27] carefully studied the details of tensile stress–strain curves, to gain insight into the fundamental mechanisms that influence fatigue behaviour and give rise to the differences observed in Figure 13. They measured the proportional stress limit (σ_{pr}) and the critical stress to induce the martensitic transformation (σ_M) and corresponding strains, as schematically illustrated in Figure 14. Below the proportional limit strain (ε_{pr}) there is pure elastic deformation, whereas between ε_{pr} and the elastic limit strain (ε_e) there is an elastic deformation, including microscopic local twinning or microscopic

local stress-induced transformation. The authors further note that the difference between ε_{pr} and ε_e is small below A_f and increases with increasing temperature above A_f, especially for the Ti-50.0at%Ni alloy.

The differences in the fatigue behaviour of these wires can be further understood by considering the mechanisms of the phase deformation. Above A_f, deformation occurs by stress-induced martensite, which is the most severe among the modes tested. Between A_s and A_f deformation is partial stress-induced martensite and partial twinning of the martensite. Testing just below A_s gives rise to a different mode of deformation. In this case, the first cycle is stress-induced martensite, followed by twinning of the martensite. At the lowest test temperatures, deformation is accommodated by martensitic twinning. It is interesting that the fatigue-crack propagation behaviour of Ti–Ni alloys is also differentiated by the details of the deformation mode. Dauskardt *et al.* [29] observed that fatigue-crack growth rates were much slower in fully martensitic Ti–Ni alloys than in alloys that undergo a stress-induced transformation.

Since Nitinol alloys perform better under strain control than under load control, most fatigue studies plot fatigue life as a function of strain, as shown in Figure 13. However, deformation stresses also affect fatigue life, so it is also necessary to compare the fatigue behaviour in terms of stress. In particular, the stress endurance limit for the alloys can be related to the test temperature. For example, the Ti-50.9at%Ni fatigue data from Figure 13 are re-plotted in Figure 15 as a function of stress. The stress endurance limits from both alloys show a linear relationship when

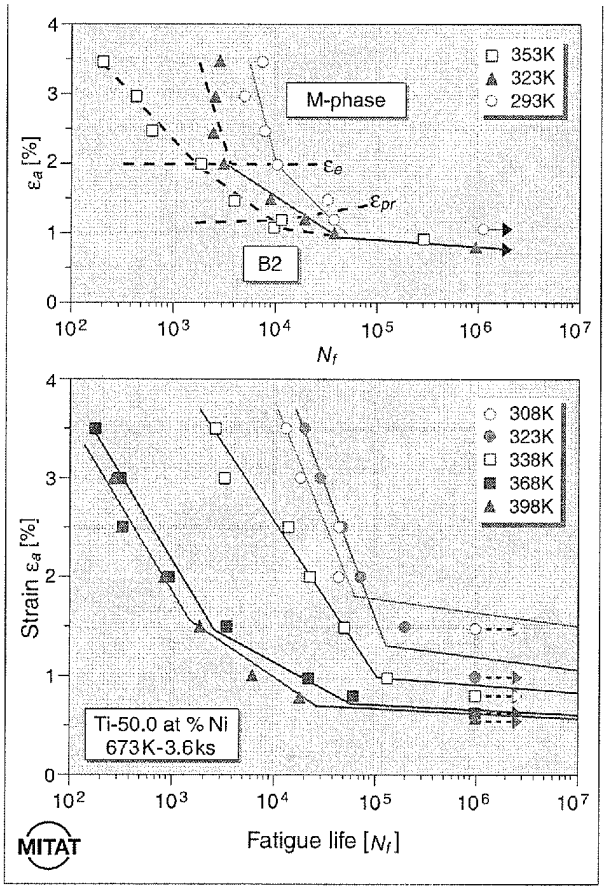

Figure 13. This figure shows the effect of applied strain on the rotary bending fatigue life for Ti-50.9at%Ni (top) and Ti-50.0at%Ni (bottom) alloys at various test temperatures. The endurance limit tends to increase with decreasing test temperature. (After Miyazaki *et al.* Refs 26 and 27.)

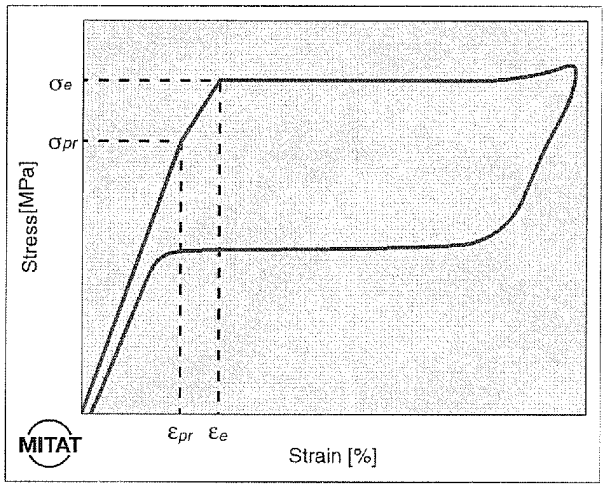

Figure 14. A schematic stress–strain curve of a superelastic Ni-Ti alloy that illustrates the proportional stress limit (σ_{pr}) and the critical stress to induce the martensitic transformation (σ_M) and corresponding strains.

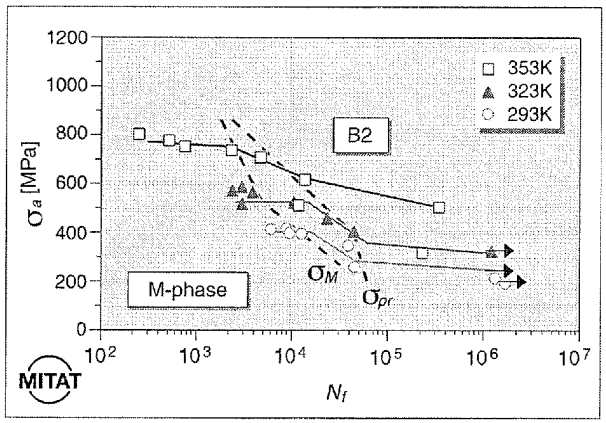

Figure 15. The data from Figure 13 are re-plotted to show the influence of stress on the fatigue life of Ti-50.9at%Ni alloys. Note that the stress endurance limit is a function of test temperature. The proportional stress limit (σ_{pr}) and the critical stress to induce the martensitic transformation (σ_M) are indicated on the figure. (After Kim and Miyazaki, Ref. 26.)

plotted against the difference between test temperature and transformation temperature, T-A_f. As highlighted by Stöckel [2], analysis of the delta between the test temperature and transformation temperature can be a powerful design tool. For example, we can extrapolate the data from constant A_f material tested at different temperatures to understand the behaviour of different transformation temperatures at a constant (body) temperature.

Conclusions

The goals of this paper were to correlate the properties of Ti–Ni alloys with processing, and to address three relevant questions frequently posed by design engineers. Optimised Ti-50.8at%Ni wire was manufactured according to industry standards by precise control of the composition, cold work and continuous strain-age annealing. We can summarise the details presented here by answering the questions posed in the introduction:

Are the mechanical properties constant over a wide range of temperatures?

As shown in Figure 5, the mechanical properties vary over a 300°C temperature range (−100°C to 200°C). Measurement of the permanent set provides a 'superelastic window' where there is minimal residual strain. Within this window, it was also demonstrated that the plateau stresses are directly related to the test temperature and transformation temperature. Therefore, the plateau stress of wire can be readily determined for a given A_f temperature. It was also discussed that the corollary is also true: for a given test temperature, the plateau stresses can be calculated for wires with different transformation temperatures. The important message from this is that the A_f, test temperature, and wire 'stiffness' can not be manipulated independently.

Can we adjust the transformation temperature without modifying the mechanical properties?

As discussed in the previous question, thermal treatments that modify the A_f temperature will also affect the other mechanical properties, especially the plateau stresses. It was shown, however, that the transformation temperature, and hence the properties, can be accurately tuned by selective ageing treatments.

Do the shape-memory and superelastic properties imply that Nitinol has an infinite fatigue life?

The fatigue properties of Ti–Ni wire were shown to depend on the mode of deformation, which, in turn, is a function of the relative stress, strain and test temperature. Higher endurance limits were found for the lowest test temperature conditions. It is recommended that fundamental fatigue tests be run in conjunction with pulsatile testing of medical devices.

References

1 Hunter JG, Sackier JM. In: Hunter JG, Sackier JM, editors. *Minimally invasive surgery*. New York: McGraw-Hill, 1993: 3.

2 Stöckel D. Nitinol medical devices and implants. *Min Invasive Ther Allied Technol* 2000; **9**.

3 Frank TG, Xu W, Cuschieri A. Instruments based on shape memory alloy properties for minimal access surgery: interventional radiology and flexible endoscopy. *Min Invasive Ther Allied Technol* 2000; **9**.

4 Funakubo H, ed. *Shape memory alloys*, New York: Gordon and Breach Science Publishers, 1984.

5 Duerig TW, Melton KN, Stöckel D, Wayman CM, editors. *Engineering aspects of shape memory alloys*. London: Butterworth-Heinemann, 1990.

6 Schüßler A. In: Pelton AR, Hodgson D, Russell SM, Duerig T, editors. *Proceedings 2nd International Conference on Shape Memory and Superelastic Technologies (SMST);* Pacific Grove: MIAS, 1997: 143–8.

7 Buchaillot L, Nakamura Y, Ataka M, Fujita H. In: Pelton AR, Hodgson D, Russell SM, Duerig T, editors. *Proceedings 2nd International Conference on Shape Memory and Superelastic Technologies (SMST);* Pacific Grove: MIAS, 1997: 183–6.

8 Hodgson D, Russell SM. Nitinol melting, manufacture and fabrication. *Min Invasive Ther Allied Technol* 2000; **9**:

9 Harrison JD. In: Duerig TW, Melton KN, Stöckel, Wayman CM, editors. *Engineering aspects of shape memory alloys*. London: Butterworth-Heinemann, 1990: 106–111.

10 Yu W. The application of thermal analysis in the study of ni-ti shape memory alloys. In: Shull RD and Joshi A, editors. *Thermal analysis in metallurgy*. Warrendale, PA: AIME, 1992: 187–204.

11 Marquez J, Slater T, Sczerzenie F. Determining the transformation temperatures of niti alloys using differential scaning calorimetry. In: Pelton AR, Hodgson D, Russell SM, Duerig T, editors. *Proceedings 2nd International Conference on Shape Memory and Superelastic Technologies (SMST);* Asilomar 1997: 13–18.

12 Chen JT, Duerig TW, Pelton AR, Stöckel D. An apparatus to measure the shape memory properties of nitinol tubes for medical applications. *J de Physique IV Coll C8*: 5: 1247–52.

13 Rice C and Sczerzenie F. Design and performance of a functional A_f tester. In: Pelton AR, Hodgson D, Russell SM, Duerig T, editors. *Proceedings 2nd International Conference on Shape Memory and Superelastic Technologies (SMST);* Pacific Grove: MIAS, 1997: 19-22.

14 Otsuka K. Introduction to the r-phase transition. In: Duerig TW, Melton KN, Stöckel D, Wayman CM, editors.

Engineering aspects of shape memory alloys. London: Butterworth-Heinemann, 1990: 36–45.
15 Tamura I, Wayman CM. Martensitic transformations and mechanical effects. In: Olson GB and Owen WS, eds. *Martensite*. ASM International, 1992: 227–42.
16 Shimizu K, Tadaki T. Shape memory effect: mechanism. In: Funakubo H, ed. *Shape memory alloys*, New York: Gordon and Breach Science Publishers, 1984: 1–60.
17 Stöckel D,Yu W. Superelastic ni-ti wire. *Wire J Int* 1991; 45–50.
18 Duerig TW, Zadno R. An engineer's perspective of pseudoelasticity. In: Duerig TW, Melton KN, Stöckel D, Wayman CM, editors. *Engineering aspects of shape memory alloys*. London: Butterworth-Heinemann, 1990: 369–93.
19 Miyazaki S. Thermal and stress cycling effects and fatigue properties of ni-ti alloys. In: Duerig TW, Melton KN, Stöckel D, Wayman CM, editors. *Engineering aspects of shape memory alloys*. London: Butterworth-Heinemann, 1990: 394–413.
20 Nishida M, Wayman CM, Honma T. Precipitation processes in near-equiatomic tini shape memory alloys. *Met Trans* 1986; **17A**: 1505–15.
21 Aaronson H, Lee Y, Russell KC. Diffusional nucleation and growth. In: Russell KC, Aaronson HI, editors. *Precipitation processes in solids*, Warrendale, PA: AIME, 1978: 31–86.
22 Melton KN. Ni-Ti based shape memory alloys. In: Duerig TW, Melton KN, Stöckel D, Wayman CM, editors. *Engineering aspects of shape memory alloys*. London: Butterworth-Heinemann, 1990: 21–35.
23 *Guidance for the submission of research and marketing applications for interventional cardiology devices*. US Department of Health and Human Services, FDA 1995.
24 Pedersen OM, Aslaksen A, Vik-Mo H. Ultrasound measurement of the luminal diameter of the abdominal aorta and iliac arteries in patients without vascular disease. *J Vasc Surg* 1993; **17**: 596–601.
25 Melton KN, Mercier O. Fatigue of niti thermoelastic martensites. *Acta Metall* 1979; **27**: 137–44.
26 Kim YS, Miyazaki S. Fatigue properties of ti-50.9at%ni shape memory wires. In: Pelton AR, Hodgson D, Russell SM, Duerig T, editors. *Proceedings 2nd International Conference on Shape Memory and Superelastic Technologies (SMST);* Pacific Grove: MIAS, 1997: 473–7.
27 Miyazaki S, Mizukoshi K, Mizukoshi, *et al*. Fatigue life of ti-50at%ni and ti-40ni-10cu(at%) shape memory alloy wires. *Mat Sci Eng A* 1999; **273–275**: 658–63.
28 Glenn R, Lee J. Accelerated pulsatile fatigue testing of ni-ti coronary stents. In: Pelton AR, Hodgson D, Russell SM, Duerig T, editors. *Proceedings 2nd International Conference on Shape Memory and Superelastic Technologies (SMST);* Pacific Grove: MIAS, 1997: 585–90.
29 Dauskardt RH, Duerig TW, Ritchie RO. Effects of *in-situ* phase transformations on fatigue-crack propagation in titanium-nickel shape memory alloys. *MRS Intl Mtg Adv Mat* 1989: **9:** 243–9.